Title: Simultaneous Quantification of Bisphenol A, Its Glucuronide Metabolite, and Commercial Alternatives by LC-MS/MS for In Vitro Skin Absorption Evaluation

Authors: Reale E, Fustinoni S, Mercadante R, Polledri E, Hopf N

Journal: Chemical Research in Toxicology

Year: 2020

Issue: 33

Volume: 9

Pages: 2390-2400

DOI: 10.1021/acs.chemrestox.0c00148

Simultaneous Quantification of Bisphenol A, Its Glucuronide Metabolite and Commercial Alternatives by LC-MS/MS for *In Vitro* Skin Absorption Evaluation

Elena Reale[a], *Silvia Fustinoni*[b,c], *Rosa Mercadante*[c], *Elisa Polledri*[c], *Nancy B. Hopf*[*a,d]

[a] Center for Primary Care and Public Health (Unisanté), University of Lausanne, Route de la Corniche 2, 1066 Epalinges, Switzerland. Elena.Reale@unisante.ch, Nancy.Hopf@unisante.ch

[b] Environmental and Industrial Toxicology Unit, Fondazione IRCCS Ca' Granda Ospedale Maggiore Policlinico, Via S. Barnaba 8, 20122 Milan, Italy. silvia.fustinoni@unimi.it

[c] EPIGET - Epidemiology, Epigenetics, and Toxicology Lab, Department of Clinical Sciences and Community Health, Università degli Studi di Milano, Via S. Barnaba 8, 20122 Milano, Italy. silvia.fustinoni@unimi.it, rosa.mercadante@unimi.it, elisa.polledri@unimi.it

[d] SwISS Centre for Applied Human Toxicology (SCAHT), MISSionsstrasse 64, 4055 Basel, Switzerland

Abstract

Bisphenol A (BPA) is the most used color developer in thermal paper products such as cashiers' receipts, followed by Bisphenol S (BPS), Wincon 8 (D-8), and Pergafast 201 (PF201). These chemicals can migrate from the paper onto the skin and possibly be absorbed and metabolized. Until now, D-8 and PF201 have not been analyzed in biological matrices, nor has a method been developed to simultaneously quantify them even though they are often found as mixtures. Our aim was to develop and validate a method to quantify BPA, its glucuronide metabolite (BPA-G), BPS, D-8 and PF201 in *in vitro* skin absorption samples. After solid-phase extraction and reversed-phase chromatography, we quantified the substances in saline that had been in contact with human dermis for 24 h using a triple quadrupole mass detector equipped with an electrospray ionization source. We assessed the method in three *in vitro* skin absorption assays using *ex-vivo* human skin from one skin donor per test substance. The quantification ranges of our method were 0.2 - 200 µg/L for BPA and 0.2 - 20 µg/L for BPA-G, BPS, D-8, and PF201. Accuracies were within ±8% of nominal concentrations. Intra-day and total precisions (%RSD) were <10% for all analytes, except for BPA in low-concentration quality control solutions (low QCs) (12.2% and 15.5%, respectively). Overall, the process efficiency was 100-113% for all analytes, except BPS low and high QCs (80% and 71%, respectively) and BPA low QCs (134%). The absorbed dose ranged from 0.02% to 49% depending on the test substance, and was not determinable for PF201. This is the first analytical method to quantify simultaneously BPA, BPA-G, and BPA alternatives in saline from *in vitro* skin absorption samples.

Introduction

Bisphenol A (BPA) is a high production volume chemical and an endocrine disruptor [1–4]. It is mainly used in polycarbonate plastics and epoxy resins. Typical products are food containers, inside liners in canned food and cash register receipts. BPA is the color developer of the thermal papers [5–9] used for cash register receipts and can migrate from the paper onto the skin when handled[10]. Ndaw and co-workers [11,12] reported a significant increase in urinary total (free + conjugated) BPA and Bisphenol S (BPS) concentrations among cashiers handling thermal paper receipts.

Due to its endocrine-disruptive effects and possible skin exposures, BPA has been gradually replaced in thermal papers by alternative substances such as BPS, Wincon 8 (D-8), and Pergafast 201 (PF201). [8,13–16] BPS is a bisphenol, D-8 is a phenol, and PF201 is phenol-free (Table 1). Based on limited *in vitro* assays, BPS acts as a weak estrogen and its endocrine activity is less than that of BPA [15], D-8 acts as an estrogen antagonist [17], and PF201 does not have any estrogenic activity [18]. The U.S. EPA [18] assessed the human health hazards associated with BPA alternatives in thermal paper, and designated these as high concerns for repeated dose toxicity (BPS) and developmental toxicity (PF201).

Several studies have focused on assessing *in vitro* BPA skin absorption and metabolism. [19–23] BPA is metabolized to its glucuronide conjugate (BPA-G) in the skin. [23] BPA metabolism is important because BPA's conjugated metabolites lack estrogenic activity. [24] Comparably to BPA, BPS undergoes phase II metabolism [25,26] and the BPS-glucuronide does not activate hormone receptors. [26] To our knowledge, there are no studies on D-8 and PF201 metabolism. BPA can penetrate the skin and reach the systemic circulation. Only one study exists on BPS *in vitro* skin absorption, [27] and none for D-8 or PF201. Skin absorption data are necessary to assess cashiers' exposures to these substances from handling thermal papers. This will ultimately help in developing risk assessments and assessing health risks in populations with exposures to BPA, BPS, D-8, and PF201.

Skin absorption studies are generally performed either on animals or *in vitro*. A chemical's ability to permeate skin is measured in *in vitro* skin experiments, which consist of a donor and receptor chamber separated by the skin membrane. The chemical of interest is applied onto the skin in the donor chamber, and the chemical and/or its metabolites are quantified in the receptor fluid. A frequently used receptor fluid is saline (0.9% w/v NaCl). Extensive literature exists on the quantification of BPA and BPS in matrices such as urine, blood, tISSues, maternal milk, food, drinks, and surface water.[12,25,28–32] BPA-G and other BPA conjugated metabolites are usually measured indirectly after enzymatic hydrolysis in urine by measuring the unconjugated BPA and expressed as total BPA (total - unconjugated = conjugated). Commercial BPA-G as well as labeled standards have become available. These have made it possible to directly quantify BPA-G in biological matrices.[33]

Solid-phase extraction (SPE) coupled with liquid chromatography-tandem mass spectrometry (LC-MS/MS) achieves the best sensitivity for quantification of BPA and its conjugated metabolites in biological matrices.[29–31,33–35] This is also true for BPS, D-8, and PF201 extracted in methanol from thermal paper.[13,15,36] Other analytical instruments have been used for bisphenols, such as high-performance liquid chromatography (HPLC) with fluorescence [20,37] or diode-array detection (DAD).[14,38,39] A few previously published articles described D-8 and PF201 analyses in methanol. The focus of these studies was to determine D-8 and PF201 concentration by direct extraction from thermal papers.[8,13–15,36] To our knowledge, no study has quantified BPA alternatives in liquid matrices similar to biological fluids. Furthermore, these color developer substances are often found as mixtures and analytical methods that could quantify them simultaneously would therefore be advantageous.

Our aims were first to develop a sensitive analytical chemical method to quantify simultaneously BPA, BPA-G, BPS, D-8, and PF201 in saline using LC-MS/MS, and then to validate this novel method with samples obtained from *in vitro* skin absorption experiments.

Experimental Procedures

Materials and Chemicals

BPA, BPA-G, and BPS were purchased from Sigma-Aldrich Chemie GmbH, Buchs, Switzerland. D-8 and PF201 were bought from Santa Cruz Biotechnology, Heidelberg, Germany. Bisphenol A-D6 (BPA-[D_6]) and bisphenol A-$^{13}C_{12}$ β-D-glucuronide (BPA-G-[$^{13}C_{12}$]) were obtained from Toronto Research Chemicals, Toronto, ON, Canada. The CAS Registry Numbers, chemical structures, and molecular weights of the analytes and the internal standards used for quantification are shown in Table 1.

LC/MS-grade acetonitrile, methanol (MeOH), and water were obtained by Carlo Erba Reagents, Milan, Italy. Saline was prepared by dISSolving 0.9% (w/v) sodium chloride (purISSim. p.a. ≥ 99.5%, supplied by Sigma-Aldrich Chemie GmbH, Buchs, Switzerland) in Milli-Q water (Millipore, Milford, MA, USA). Ammonium hydroxide solution (NH4OH ≥ 25% in water, eluent additive for LC-MS) was supplied by Sigma-Aldrich Chemie GmbH, Buchs, Switzerland.

Standard Solutions

A stock solution (1 mg/mL) was prepared in LC-MS-grade MeOH for BPA, BPA-G, BPS, D-8, and PF201, as well as for the internal standards BPA-[D6] and BPA-G-[$^{13}C_{12}$]. Two intermediate solutions containing all five analytes at 200 µg/L and 2 µg/L were prepared by dilution of the stock solutions in saline. Six calibration standard solutions ranging from 0.02 to 200 µg/L were obtained by diluting intermediate solutions in saline. Quality control solutions (QCs) were prepared at 0.4 µg/L (low QC) and 10 µg/L (high QC) in saline. A mixed internal standard solution (ISS) containing BPA-[D_6] and BPA-G-[$^{13}C_{12}$] was prepared in saline (10 mg/L). Stock solutions of BPA, BPA-G, BPS and D-8 and intermediate solutions were stored at -20°C for up to 6 months. As PF201 was stable in water and unstable in MeOH, PF201 stock solution had to be freshly prepared when new intermediate solution was needed. Calibration standard solutions were freshly prepared from intermediate solutions on every analysis day.

Solid-phase Extraction (SPE)

Calibration standard solutions, QC solutions, and samples (3 mL) were spiked with 15 µL of the ISS and then directly loaded onto SPE cartridges (Isolute C18 200 mg/6 mL; Biotage AB, Uppsala, Sweden). SPE cartridges were previously conditioned with 2 mL of MeOH , and equilibrated with 2mL of water. After washing (2 x 2 mL water), the analytes were eluted (2 x 2 mL MeOH) through a polytetrafluoroethylene filter (PTFE, 0.45 µm, 4 mm diameter; BGB Analytik, Switzerland). Conditioning, equilibration, washing, and elution were carried out using a manifold system (Pressure+, Biotage AB, Uppsala, Sweden). The eluate was evaporated to dryness under a nitrogen stream, and the residue was dISSolved in 300 µl of water.

Table 1. Chemical structures, molecular weights (MW), retention times, retention time variability (%RSD), collision energies, and multiple reaction monitoring (MRM) transitions for the detection and quantification of the different analytes.

Compound	Acronym	CAS n°	MW	Structure	Retention time (min)	%RSD retention time	MRM transitions[a]		Collision energy (eV)[a]
							Precursor ion	Product ion	
Bisphenol A	BPA	80-05-7	228.29	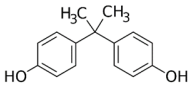	5.0	0.2	227.1	212.4	16
							227.1	133.1	23
Bisphenol A-d_6	BPA-d_6	86588-58-1	234.32	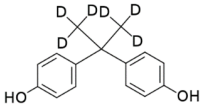	5.0	0.2	233.1	138.1	27
							233.1	93.1	31
Bisphenol A mono-β-D-glucuronide	BPA-G	267244-08-6	404.41	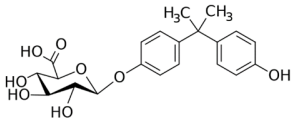	3.5	0.3	403.7	228.1	26
							403.7	113.1	15
Bisphenol A-$^{13}C_{12}$ β-D-Glucuronide	BPA-G-$^{13}C_{12}$	1313730-08-3	416.32	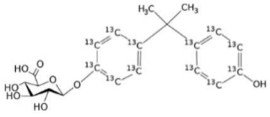	3.5	0.2	415.2	239.1	26
							415.2	113.1	15
Bisphenol S	BPS	80-09-1	250.27	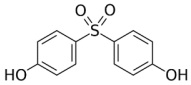	0.5	1.7	249.0	108.0	27
							249.0	156.0	21
Wincon 8	D-8	95235-30-6	292.35	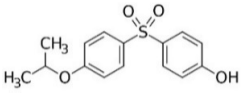	3.8	0.1	291.0	248.0	21
							291.0	184.0	29
Pergafast 201	PF201	232938-43-1	460.52	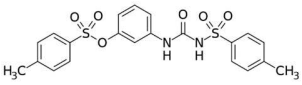	3.8	0.1	459.2	170.0	19
							459.2	106.0	41

[a] Data in bold are for quantifiers, other data are for qualifiers.

LC-MS/MS

Calibration standard solutions, QC solutions or samples were injected (10 µl) in the LC system (UltiMate 3000 HPLC system, Thermo Fisher, Fisher Scientific, Reinach, Switzerland) equipped with a packed column (C18 column, 100 x 2.1 mm, 1.8 µm, Eclipse Plus, Zorbax, Agilent Technology, Basel, Switzerland) kept at 40°C. The mobile phase was a mixture of water and acetonitrile, each containing 5 mM of ammonium hydroxide, operating at a flow rate of 0.4 mL/min with the following gradient: 98% water (0.5 min); decreased to 50% water (1 min); 50% water (2 min); increased to 98% water (1 min), and 98% water (3 min).

A triple-quadrupole mass spectrometer (MS/MS) equipped with a heated electrospray ionization (H-ESI) source (TSQ Quantiva, Thermo Fisher, Fisher Scientific, Reinach, Switzerland) was used for detection. The MS conditions were optimized as follows: spray voltage, -3300 V; sheath gas, auxiliary gas, and

sweep gas pressures of 25, 13, and 0 respectively (arbitrary units); ion transfer tube temperature, 298°C; and vaporizer temperature, 270°C. The MS/MS system was set on multiple reaction monitoring (MRM), with the H-ESI source in negative ion mode. Peak integration, MS quantitation, and data processing were carried out with Thermo Scientific Chromeleon 7.2 Chromatography Data System (CDS) software.

Sample quantification

Internal calibration with isotope-labeled internal standards was used for quantification. BPA-[D_6] was used as internal standard for BPA, while BPA-G-[$^{13}C_{12}$] was used as internal standard for BPA-G, BPS, D-8, and PF201. Calibration curves were obtained by analyzing the calibration standard solutions in saline containing ISS. The calibration plot of standard/internal standard peak areas ratios (y) versus calibration standard nominal concentrations (x) was fitted by least-squares linear regression with a weighting factor of 1/x.

Method development

The following parameters were studied to SPE conditions: SPE cartridge types and sizes for maximum retention and minimum BPA contamination from cartridge plastics; BPA presence in the solvents used for analyses; wash and elution solvent volumes; and number of wash and elution steps to yield the maximum recovery. MS conditions, MRM transitions, and collision energies were optimized combining autotuning and manual tuning of a 5 mg/L aqueous standard solution directly infused in the MS system without passing through the LC. LC conditions were optimized by testing several different columns as well as different mobile-phase solvents and gradients. The following LC columns were tested for method development were the Hypersil Gold PFP (50 x 2.1 mm, 3 µm, Thermo), Acquity UPLC HSS T3 (75 x 2.1 mm, 1.8 µm, Waters), Zorbax Eclipse Plus C18 (100 x 2.1 mm, 1.8 µm, Agilent), Zorbax Eclipse XDB-C8 (150 x 2.1 mm, 3 µm, Agilent), Hypersil Gold Phenyl (50 x 2.1 mm, 1.9 µm, Thermo), XBridge - RP18 (50 x 4.6 mm, 3.5 µm, Waters), Acquity BEH C18 (50 x 2.1 mm, 1.7 µm, Waters), Synergi Hydro RP (75 x 3 mm, 4 µm, Phenomenex), Synergi MAX – RP (75 x 3 mm, 4 µm, Phenomenex), Gemini-NX C18 (30 x 4.6 mm, 3 µm, Phenomenex), ODP2 HP-2D (150 x 2.0 mm, 5 µm, Shodex).

Method validation

Validation of the optimized method included five runs carried out on 5 days over a 2-week period. Four concentrations were prepared and quantified in triplicate in each run: the two lowest calibration standards (0.02 and 0.2 µg/L), and the low and high QC solutions. Calibration curves were generated and linearity assessed by means of their coefficient of determination (R^2). Slope variability was calculated as the standard deviation of five slopes expressed in % of the mean (coefficient of variation or relative standard deviation, %RSD). The lower limit of quantification (LLOQ) was defined as the lowest concentration on the calibration curve that could be quantified within 30 % of relative bias (% of nominal concentration) and precision (%RSD) during validation. Precision and accuracy were calculated for the low and high QC solutions. Acceptance threshold for accuracy and precision was 20%. Accuracy or relative bias was calculated as the percent ratio of the mean concentration to the nominal concentration. Precision was calculated as intra-day precision (repeatability) and intermediate precision. These were determined with an ANOVA-based variance decomposition, and they were expressed as %RSD. For intra-day precision, %RSD was calculated as the square root of the intra-day variance, divided by the mean of all results. [40] The intra-day variance (s_r^2) was calculated as the mean of the daily variances (eq. 1):

$$s_r^2 = \frac{\sum_{d=1}^{D}\sum_{r=1}^{n}(x_{dr}-\bar{x}_d)^2}{D\,(n-1)} \qquad (1)$$

where D is the total number of days, n is the number of replicates per day, x_{dr} is the result for replicate r on day d and $\bar{x}_d$ is the average of all replicates on day d.

For intermediate precision, %RSD was calculated as the square root of the total variance s_R^2 divided by the mean of all results. The total variance s_R^2 was calculated as the sum of the intra-day variance s_r^2 and the between-day variance s_g^2 (eq. 2) [40]:

$$s_R^2 = s_r^2 + s_g^2 \text{ (if } s_g^2 \geq 0\text{)} \qquad (2)$$

$$s_R^2 = s_r^2 \text{ (if } s_g^2 < 0\text{)}$$

$$s_g^2 = \frac{\sum_{d=1}^{D}(\bar{x}_d - \bar{\bar{x}})^2}{D-1} - \frac{s_r^2}{n}$$

where $\bar{\bar{x}}$ indicates the average of all results.

Matrix effect, extraction recovery, and process efficiency were evaluated using the method of Matuszewski and co-workers [41] for five replicates of low and high QC solutions. Matrix effect (ME%) was calculated as the percent peak area ratio of QC solutions where the analytes were spiked after the SPE and QC solutions prepared in neat reconstitution solvent (water). Extraction recovery (RE%) was calculated as the percent peak area ratio of QC solutions spiked before and after the SPE. Process efficiency (PE%) was calculated as the product of matrix effect and extraction recovery.

The use of pure saline as a surrogate matrix for the preparation of calibration standards and QCs was evaluated. Three different matrices, consisting of saline that had been in contact with three different dermis specimens for 24 h, were used to prepare three calibration curves. The mean slope of these calibration curves was compared with the mean slope of calibration curves (n=3) prepared in pure saline.

Specificity was assessed by verifying the absence of interfering peaks in five different blank samples. Blank samples were composed of saline that had been in contact with human dermis from five different skin donors for 24 h during skin absorption experiments (see 'Skin absorption experiments').

Carry-over is a systematic error that is derived from the analytes' signals from a preceding sample introduced into the next sample, and was assessed by injecting four blanks immediately following the 200 µg/L calibration standard. Carry-over was calculated as the mean percent ratio of the analytes' peak areas in each blank over the LLOQ peak area (n = 8).

The stability of analytes in aqueous solutions and in matrix was studied. All spiked aqueous and matrix solutions for stability testing were prepared in duplicates. For aqueous solutions, stability was assessed by comparing the area under the peak of a freshly prepared aqueous solution containing all analytes (5 mg/L) with that of stored solutions at varying temperatures and times. These solutions were diluted 100 times before they were injected in the LC system. For analytes in matrix, stability was assessed by comparing the concentration of a freshly prepared matrix solution containing all analytes (10 µg/L) with that of stored matrix solutions at varying temperatures and times.

Skin absorption experiments

Samples from skin absorption experiments were analyzed to test the efficiency of the developed LC-MS/MS method. Skin absorption and metabolism were measured *in vitro* using diffusion cells.[42] In each cell a human skin flap separates a donor chamber, where the tested chemical is applied, and a receptor fluid, into which the tested chemical migrates after diffusing through the skin. In our experiments we used

flow-through diffusion cells (11.28 mm internal diameter, 1 cm^2 area, PermeGear, obtained from SES Analytical System, Bechenheim, Germany), and saline as receptor fluid. Saline was continuously stirred and pumped (50 µL/min; peristaltic pump from Ismatec IPC-N, IDEX Health and Science GmbH, Wertheim-Mondfeld, Germany) through the receptor chamber. Cells were kept at 32°C by a heated water-bath circulator (Haake SC 100 Digital Immersion Circulator, 100°C w/cla, Thermo Scientific, Newington, NH, USA). *Ex-vivo* full thickness human abdominal skin was obtained immediately following surgery from the Plastic and Reconstructive Surgery Department (DAL) at the Centre Hospitalier Universitaire Vaudois (CHUV, Lausanne, Switzerland) (ethical protocol 264/12). Skin was rinsed with saline and dermatomed (AcculanII, B. Braun/Aesculap, Sempach, Switzerland) to 800 µm thickness. The skin was then cut into circular sections and mounted onto the flow-through diffusion cells with the stratum corneum side facing up. After a 30-min stabilization period, the skin flaps were exposed to 100 µL of test solutions for 24 h. Test solutions of BPA, BPS, D-8 and PF201 were prepared in water (250 mg/L, 250 mg/L, 20 mg/L and 3 mg/L, respectively). Their concentrations were verified using the analytical method described here for saline except for three steps: the test solutions were not extracted (SPE), calibration standards were prepared in water, and external calibration was used for quantification. Each substance was tested in three *ex-vivo* human skin flaps (n=3) from one skin donor (N=1). Trans-epidermal water loss (TEWL) (VapoMeter wireless, Delfin Technologies Ltd., Kuopio, Finland) was tested after the 30-min stabilization period as well as at the end of each experiment to confirm skin integrity throughout the whole experiment. Skin flaps with a TEWL greater than 11 $g/m^2/h$ were excluded.[43] Receptor fluid was sampled by a fraction collector (FC 204, Gilson Inc., Middleton, WI, USA) at several time intervals over 24 h. Receptor fluid samples were quantified using the developed analytical method. The analyte concentration was set at LLOQ/2 whenever the analysis resulted in a value below the lower limit of quantification (<LLOQ). If two out of the three skin flaps tested per substance at any time point give < LLOQ results, then the mean analyte concentration was set as < LLOQ at that time point.

Results

Analytical method development and validation

Analytical column, SPE, and solvents. The first HPLC columns tested for method development were the Thermo Hypersil Gold PFP, Waters Acquity UPLC HSS T3, and Agilent Zorbax Eclipse Plus C18. The best analyte separation, peak shapes, and peak intensities were observed with the Zorbax Eclipse Plus C18 column, but BPS was not retained (retention time (RT) = 0.6 min). Therefore, several other chromatographic columns were tested (see 'Method development'). BPS's RT was the longest using Agilent Zorbax Eclipse XDB-C8 (1.25 min) and Shodex ODP2 HP-2D (1.5 min) columns. However, the Zorbax Eclipse XDB-C8 column had lower peak intensities compared to other columns, and the Shodex ODP2 HP-2D led to considerably worse calibration linearity. Overall, the best performance was observed using the Zorbax Eclipse Plus C18 and the Acquity BEH C18, for which BPS's RT was 0.6 and 0.3 min, respectively. Therefore, the column selected for further method development and validation was the Zorbax Eclipse Plus C18.

Several adjustments were made to the solvents used as mobile phase and in their gradient. In the literature, BPA analysis in biological matrices by LC-MS/MS often used C18 columns and water:MeOH [25,44] or water:acetonitrile mobile phases.[12,29] Therefore, both options were studied. The presence of NaCl (0.9% w/v) produced a strong ion suppression for BPA and BPA-D_6 regardless of using water:MeOH or water:acetonitrile. Working in negative ion mode and adding ammonia in the mobile phases increased the sensitivity, as it enhanced the formation of the parent ion $[M-H]^-$. However, sample preparation by SPE

was still necessary to increase the sensitivity. For the Agilent Zorbax Eclipse Plus C18 water:acetonitrile with 5 mM ammonium hydroxide was the selected mobile phase that gave well-resolved and symmetrical peaks with stable retention times. Different gradients were tested, starting from 2% to 100% organic phase and gradually reducing the organic phase span and gradient times. The final gradient gave the best compromise between resolution and run time.

Solvents and other materials used for routine analysis, such as plastic pipet tips, SPE cartridges, and PTFE filters were tested for BPA contamination. All these materials showed BPA signals ranging from 1% to 16% of the LLOQ signal. Overall, BPA signal in blank solutions was 45% of LLOQ signal. For BPA-G, BPS, D-8 and PF201, the blank solutions' signals ranged between 4% and 7%.

MS quantifiers. Table 1 shows the multiple reaction monitoring (MRM) transitions used to quantify and confirm the analytes and internal standards, the collision energies needed to produce the desired product ions, and the retention times of their chromatographic peaks. The most abundant product ion was used as the quantifier (marked in bold in the table), and the second most abundant product ion was used as the qualifier. The extracted ion chromatograms (XICs) of all five analytes are shown in Figure 1. Each chromatogram was obtained by registering the MRM transition of the molecular ion $[M-H]^-$ to produce the quantifier in blank solutions and in calibration standard solutions at the LLOQ (Figure 1).

Calibration curve and limits of quantification. Table 2 shows the calibration curve, accuracy, and precision. The lower limit of quantification (LLOQ) was 0.2 µg/L for all five analytes. The upper limit of quantification was 200 µg/L for BPA, and 20 µg/L for BPA-G, BPS, D-8, and PF201. Linearity was good with $R^2 \geq 0.998$ for all the analytes. Slope variability ($\%RSD_{slope}$) was equal to or under 8.4 for all analytes except BPS, for which $\%RSD_{slope}$ was 14.8.

Accuracy and Precision. Accuracy values were within ±8% of nominal concentration for low and high QCs of all analytes. Intra-day precision and intermediate precision were both under 10% for all analytes, except BPA low QC, where they reached respectively 12.2 % and 15.5 %.

Matrix Effect, Extraction Recovery and Process Efficiency. All results of the extraction recovery, matrix effect and overall process efficiency are listed in Table 3.

Justification of Surrogate Matrix. The slopes of the calibration curves prepared in matrix or in surrogate matrix differed by -5% for BPA, 4% for BPA-G, -16% for BPS, 8% for D-8, and 4% for PF201 (Table 4). The slope variability ($\%RSD_{slope}$) of the calibration curves in matrix was 20%, 32%, 7%, 4% and 5% for BPA, BPA-G, BPS, D-8, and PF201, respectively.

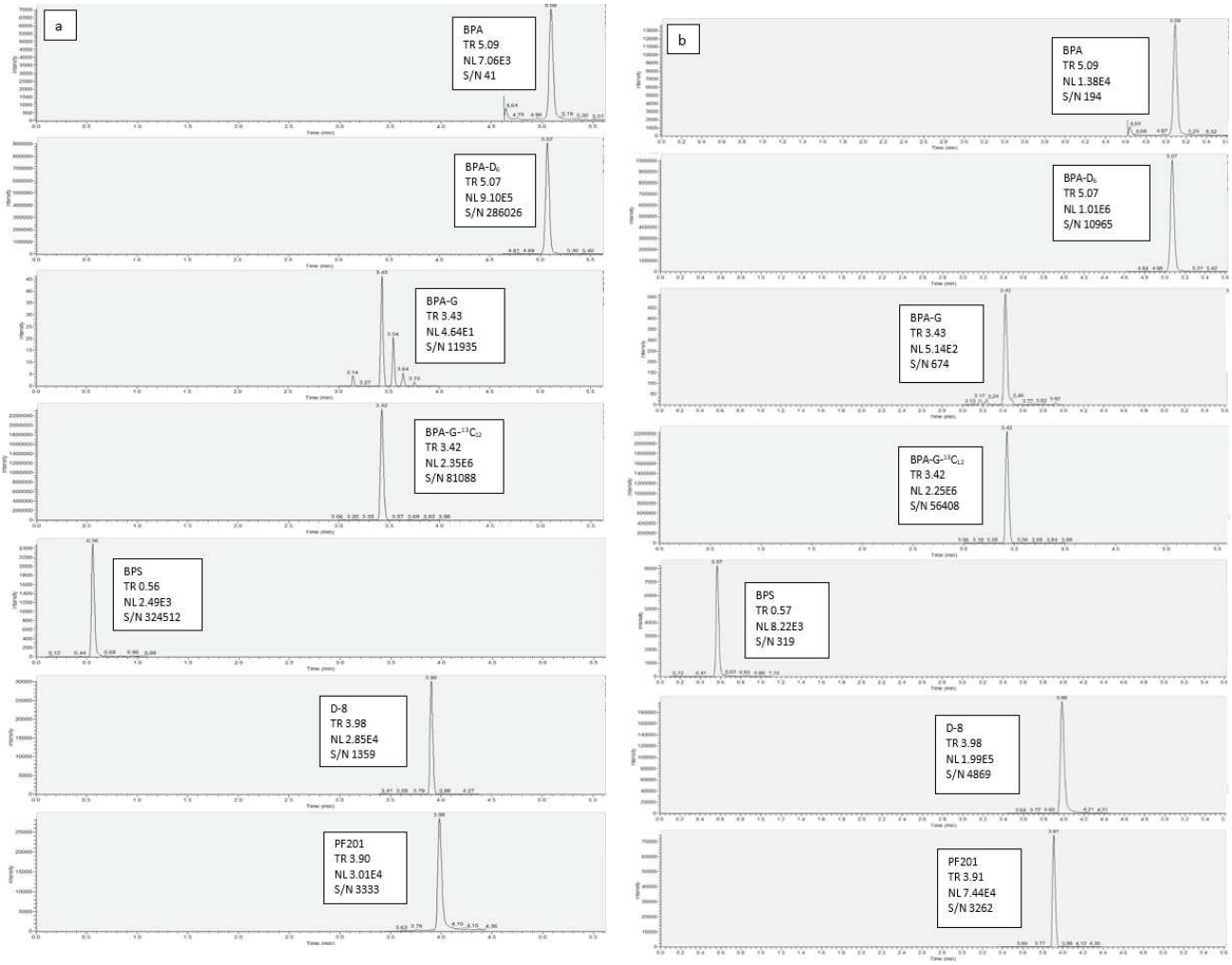

Figure 1. Extracted ion chromatograms (XICs) of BPA, BPA-D_6, BPA-G, BPA-G-$^{13}C_{12}$, BPS, D-8, and PF201 in blank solutions (a) and in calibration standard solutions at the LLOQ = 0.2 µg/L (b). TR = retention time, NL = normalization level, S/N = signal-to-noise ratio.

Table 2. Calibration curve data, including lower limit of quantification (LLOQ) and upper limit of quantification (ULOQ), and precision and accuracy of the analytical method for each investigated substance.

Analyte	Calibration curve						Accuracy (n = 15)			Precision (n = 3, 5 days)[c]					
	Investigated range (µg/L)	LLOQ – ULOQ (µg/L)	Slope	Intercept	R^2	%RSD alope	% of nominal concentration			Intra-day (%RSD)			Intermediate (%RSD)		
							LLOQ (min – max)	QC low[a] (min – max)	QC high[b] (min – max)	LLOQ	QC low[a]	QC high[b]	LLOQ	QC low[a]	QC high[b]
BPA	0.02-200	0.2-200	2.011	0.3380	0.999	4.1	118 (96 –129)	108 (91 – 122)	100 (93 – 107)	16.3	12.2	2.9	17.5	15.5	6.4
BPA-G	0.02-200	0.2-20	0.158	0.0011	0.999	8.4	102 (89 – 120)	101 (90 – 104)	93 (89 – 98)	5.3	5.1	2.8	11.9	8.5	4.5
BPS	0.02-200	0.2-20	3.144	0.0668	0.999	14.8	100 (78 – 109)	101 (94 – 105)	106 (100 – 115)	8.2	8.8	9.4	14.3	8.8	9.9
D-8	0.02-200	0.2-20	25.137	0.2656	0.999	6.8	101 (98 – 102)	104 (103 – 105)	100 (97 – 103)	3.4	3.4	3.5	3.7	3.4	3.7
PF201	0.02-200	0.2-20	11.127	0.6087	0.998	5.5	94 (81 – 101)	102 (98 – 111)	104 (101 – 107)	6.2	7.5	7.2	10.1	7.9	7.2

[a] 0.4 µg/L

[b] 10 µg/L

[c] Precision is presented as intra-day and intermediate (intra + inter-day) percent relative standard deviation (%RSD).

Table 3. Matrix effect, extraction recovery, and overall process efficiency as defined by Matuszewski et al. [41]

Analyte	Nominal concentration (µg/L)	% Extraction recovery		% Matrix effect		% Process efficiency	
		without IS	with IS	without IS	with IS	without IS	with IS
BPA	0.4	84	107	180	125	151	134
	10	82	106	107	97	87	103
BPA-G	0.4	78	88	123	123	95	108
	10	71	83	137	136	98	113
BPS	0.4	100	114	70	70	70	80
	10	90	105	69	68	62	71
D-8	0.4	97	110	100	100	97	110
	10	91	107	98	97	90	103
PF201	0.4	89	101	101	101	90	102
	10	84	98	103	101	86	100

Table 4. Justification of the use of saline as surrogate matrix for the saline that has been in contact with human dermis up to 24h.

Analyte	Slope (± SD)		% Δ[a]
	Calibration in surrogate matrix	Calibration in matrix	% relative difference of the calibration curve slopes obtained in surrogate matrix and in the real matrix
BPA	4.427 (± 0.52)	4.646 (± 0.92)	-5
BPA-G	0.094 (± 0.03)	0.090 (± 0.03)	4
BPS	2.352 (± 0.65)	2.815 (± 0.20)	-16
D-8	48.48 (± 8.49)	44.97 (± 1.60)	8
PF201	24.27 (± 5.24)	23.37 (± 1.25)	4

[a] The difference (% Δ) in mean slope of calibration curves prepared in surrogate matrix vs. matrix is shown (n = 3).

Specificity. Monitoring two transitions per analyte by the MS/MS system provided high specificity. However, as shown in Figure 1, no interferences were detected in our experimental conditions.

Carry-over. The mean (n=8) carry-over for BPA was the ratio of the BPA peak area in the blank divided by the peak area of the LLOQ. The blank was the first injected blank, after the ULOQ. Mean carry-over for BPA was 42% of the LLOQ (0.083 µg/L). The second blank was 22% (0.044 µg/L), the third was 18% (0.037 µg/L), and the fourth was 17% (0.034 µg/L). Carry-over values in the first, second, third, and fourth blanks were respectively 4%, 3%, 3%, and 4% of the LLOQ (0.007-0.008 µg/L) for BPA-G; 1%, 1%, 1%, and 1% of the LLOQ (0.001 µg/L) for BPS; 132%, 20%, 14%, and 13% of the LLOQ (0.26, 0.041, 0.029, and 0.026 µg/L) for D-8; and 14%, 12%, 11%, and 11% of the LLOQ (0.023-0.027 µg/L) for PF201.

Stability. Stability tests showed that in aqueous solution all analytes were stable for at least 7 days at room temperature. All analytes except BPA-G were stable for at least 80 days at +4 °C (Table 5). In matrix, all analytes were stable for at least 1 day at room temperature, and at least 80 days at -20 °C. Stock solutions of BPA, BPA-G, BPS, and D-8 in MeOH were stable for up to 6 months (peak area variation ± 20%). PF201 stock solution's peak area was reduced by 90% upon storage at -20°C for 6 months.

Table 5. Stability of the analytes in different matrices.

Compound	Storage conditions								
	In H_2O					In matrix			
	T_{room}		+4°C			T_{room}	-20°C		
	24h	7 days	24h	7 days	80 days	24h	3 freeze/thaw cycles (24h)	7 days	80 days
BPA	103	107	113	99	100	93	115	75	98
BPA-G	102	108	111	115	81	82	90	88	110
BPS	109	105	104	110	100	109	117	88	93
D-8	100	111	113	116	101	113	111	98	101
PF201	93	116	103	127	102	95	97	97	90

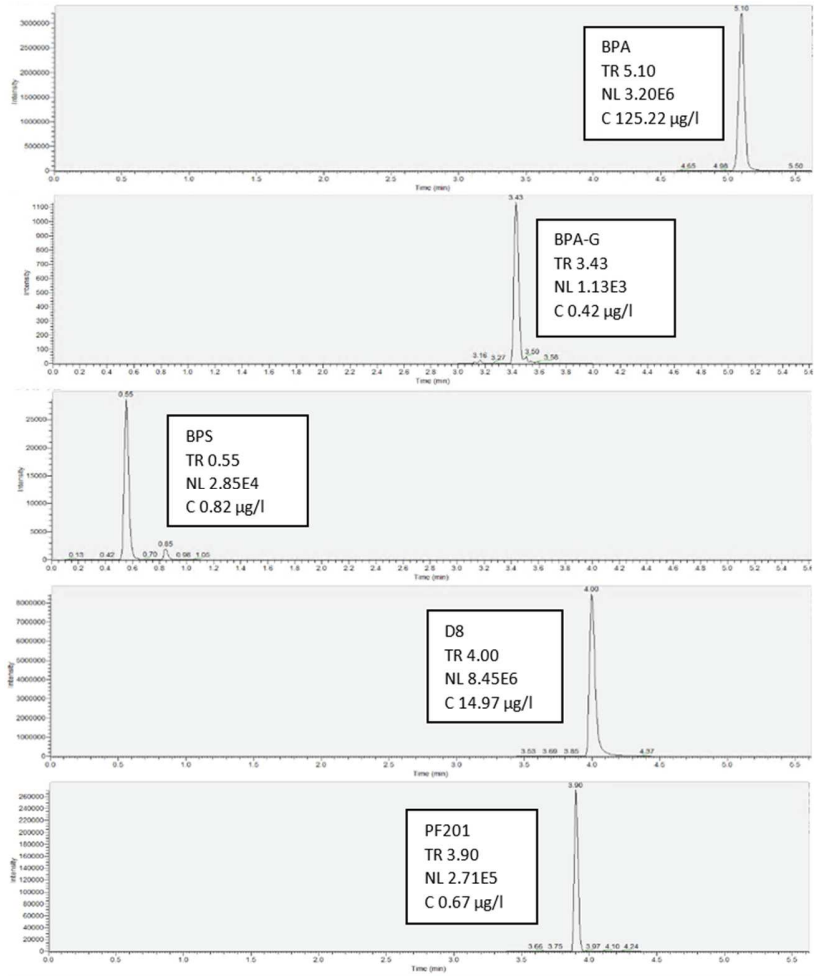

Figure 2. Extracted ion chromatograms (XICs) of BPA, BPA-G, BPS, D-8, and PF201 in a sample obtained from skin absorption experiments. TR = retention time, NL = normalization level, C = concentration.

Application of the developed method to skin absorption samples

Samples from preliminary skin absorption testing were analyzed to evaluate the analytical method's feasibility. The extracted ion chromatograms (XICs) of the analytes in our skin absorption samples are shown in Figure 2. Amounts of BPA, BPA-G, BPS, and D-8 over the LLOQ were quantified within the validated ranges (Table 6). Even though PF201 was quantified in a few samples, the overall value was < LLOQ, as two out of three repeats were <LLOQ. After 24 h of skin exposure to the test solutions, the total dose recovered in the receptor fluid was 48.6%, 0.02%, 0.08%, and 27.4% of the applied dose for BPA, BPA-G, BPS, and D-8, respectively, and was not determinable for PF201. Intra-skin absorption variability (%RSD) at the different time points ranged from 17% to 110% for BPA, 43% to 63% for BPA-G, 74% to 104% for BPS, and 9% to 66% for D-8.

Table 6. Dose recovered (% of applied dose) in receptor fluid of *in vitro* skin absorption assays sampled at different times points after the beginning of skin exposure.

Time	% of applied dose (± SD)[a]								
(h)	BPA		BPA-G		BPS		D-8		PF201
0	0.005	± 0.001	n.d.		n.d.		n.d.		n.d.
1	0.019	± 0.020	n.d.		n.d.		n.d.		n.d.
2	0.427	± 0.383	n.d.		n.d.		n.d.		n.d.
3	1.355	± 0.891	0.003	± 0.002	n.d.		0.331	± 0.220	n.d.
4	2.427	± 1.306	0.004	± 0.002	n.d.		0.881	± 0.411	n.d.
5	3.328	± 1.555	0.004	± 0.002	n.d.		1.789	± 1.141	n.d.
6	3.946	± 1.712	0.003	± 0.002	n.d.		1.872	± 0.592	n.d.
8	9.588	± 3.710	0.005	± 0.002	n.d.		5.131	± 1.820	n.d.
10	9.406	± 2.999	n.d.		0.008	± 0.007	5.730	± 1.365	n.d.
12	6.460	± 1.486	n.d.		0.010	± 0.010	4.179	± 0.776	n.d.
14	4.236	± 0.923	n.d.		0.010	± 0.008	2.688	± 0.358	n.d.
16	2.700	± 0.501	n.d.		0.011	± 0.009	1.650	± 0.155	n.d.
18	1.805	± 0.350	n.d.		0.011	± 0.008	1.102	± 0.149	n.d.
20	1.254	± 0.216	n.d.		0.010	± 0.008	0.821	± 0.117	n.d.
22	0.923	± 0.166	n.d.		0.010	± 0.007	0.639	± 0.072	n.d.
24	0.699	± 0.131	n.d.		0.009	± 0.006	0.523	± 0.075	n.d.
Total	48.578	± 14.435	0.019	± 0.010	0.080	± 0.078	27.335	± 7.020	n.d.

[a] Values are expressed as mean results ± SD (n=3). For BPA-G the dose recovered is expressed as % of BPA applied dose.

n.d. = not determinable because two or three out of three skin samples gave results of analyte concentration <LLOQ (LLOQ = 0.2 µg/L).

Discussion

We developed and validated a method for the simultaneous quantification of BPA, BPA-G, BPS, D-8, and PF201 in saline from *in vitro* skin absorption assays. Our results show that this method is selective, accurate and precise over wide concentration ranges, as well as applicable to samples from *in vitro* human skin absorption experiments.

Sample analysis without any pre-treatment was assessed. The presence of 0.9% NaCl in saline led to ion suppression and loss in sensitivity for all analytes over few analyses within the same run (data not shown). The addition of a base, such as ammonia, in the mobile phase improved the analytes' ionization and increased H-ESI response. This effect has also been reported by Furey and co-workers[45] and Tan and coworkers.[46] However, a decrease of the peak areas was observed during the analytical run. This effect was overcome by sample pre-treatment with Solid-phase extraction (SPE).

Several SPE cartridges were tested for maximum analyte retention. As BPA is used in polycarbonate plastics, SPE cartridges were also tested for possible BPA presence and leakage from the plastic. Assay

contamination by ubiquitous BPA has been reported to be an ISSue in some cases,[34,47,48] while well controlled in others.[49,50] In our studies, all cartridges had BPA concentrations below the LLOQ but still detectable. The smallest BPA peaks were detected using 6 mL cartridges. A possible explanation is that the higher capacity of 6 mL vs. 3 mL cartridges limited the contact area between the sample and the cartridge's plastic walls. Similar results were obtained using Water Oasis HLB 1 mL cartridge. The lowest BPA signals were detected using J.T. Baker Bakerbond SPE™ C18 and Biotage Isolute C18 cartridges. Isolute C18 cartridges were chosen for method development and routine analysis because they were optimal for our sample volume and were less expensive.

In method validation, the higher variability for BPA's low QC was likely due to the ubiquitous contamination of BPA. For all analytes, most of the variability derived from repeatability s^2_r, and not from the inter-day variance s^2_g. The differences in the slope of the calibration curves prepared in matrix or in surrogate matrix were not negligible, especially for BPS. They were deemed sufficiently low, however, to justify the use of saline as a surrogate matrix given the scarcity of human skin samples for skin absorption studies. The higher slope variability of BPS's calibration curves in surrogate matrix compared to the other analytes was likely due to the lack of BPS retention on the chromatographic column. Calibration slope variability higher than 5% indicates the presence of relative matrix effects [51]. The calibration slope variability in matrix was >5% for BPA, BPA-G, and BPS, while ≤5% for D-8 and PF201. This was in accordance with our matrix effect study results where no or little matrix effects were observed for D-8 and PF201. Extraction recoveries ranged between 98% and 101% for PF201 and between 107% and 110% for D-8. This resulted in a good overall process efficiency of 110 % and 103% for D-8 low and high QCs, and 102% and 100% for PF201. Less efficient was the analytical process for BPS (PE% = 80% and 71% for the low and high QCs, respectively). This was mostly due to the matrix effects, which were 70% for the low QC and 68% for the high QCs. The use of BPA-G-[$^{13}C_{12}$] as an internal standard for BPS was not able to correct for matrix effects. This was probably because of the difference in chemical structure and their retention times. Surprisingly, BPA-G-[$^{13}C_{12}$] was not able to correct for matrix effects for BPA-G either. This led to an ion enhancement of 123% and 136% for BPA-G low and high QCs respectively. BPA-G matrix effects were compensated by extraction recoveries ranging from 83% to 88%, which resulted in overall process efficiency of 108% for BPA-G low QC and 113% for BPA-G high QC. Recoveries using Biotage Isolute C18 cartridges ranged within ±10% of the nominal QC concentrations, except for BPS low QC (114%) and BPA-G high QC (83%), after optimizing the wash/eluent solvents and volume and correcting with the internal standard for all analytes. BPA isotope-labeled analogue BPA-[D_6] was able to compensate for BPA high-QCs' matrix effect (97%) and recovery (106%), leading to a high process efficiency (103%). BPA low-QCs were affected by a stronger matrix effect that the internal standard could partly correct (125%). Coupled with an extraction recovery of 107%, this led to a process efficiency of 134%. We hypothesize that the presence of ubiquitous BPA (in plastics and solvents) could be a cause of the high value observed in the matrix effect study, given the high BPA signal in blank solutions (45% of LLOQ signal for BPA, <7% of LLOQ signal for BPA-G, BPS, D-8, and PF201). This value could not justify the high matrix effect on the BPA low QCs, but indicated that BPA background contamination was still possible and could affect the results at low concentrations.

Commonly, guidelines on bioanalytical method validation[52,53] require that the analyte response in a carry-over blank is less than 20% of the LLOQ response. Therefore, three blanks should be injected for samples with BPA concentration >200 µg/L, while for D-8 at this concentration one blank is necessary. This concentration is 10 times higher than D-8's ULOQ. No carry-over blank injections are necessary for BPA-G, BPS, and PF201.

Our stability test results in aqueous solution and in matrix were similar to results obtained by Ye and co-workers.[54] They reported BPA-conjugated species in urine to be stable for at least 7 days at +4 °C, and for at least 180 days at -70°C. Our stability test results in MeOH confirm the high instability of PF201 in protic and slightly acidic solutions reported by Eckardt and Simat.[14]

Our method was applicable to *in vitro* skin absorption assays. The high intra-skin absorption variability was most likely due to the skin samples, i.e., due to possible slightly different skin thicknesses, skin elasticity, number of stretchmarks, and amount of hair. These skin permeation results are only preliminary, as they were obtained using skin samples from only one donor per test substance. Including additional skin donors is necessary to use these results for risk assessment. Even if only preliminary, our results suggest that BPA and D-8 had the highest skin absorption. This is in line with the octanol/water partition coefficient (log K_{ow}) of the test substances, which is a key parameter for the diffusion of chemicals through the stratum corneum [55]. BPA and D-8 are more lipophilic (log K_{ow} = 3.3 and 3.4, respectively) than PF201 and BPS (log K_{ow} = 1.2 and 2.6, respectively). Lipophilic substances with molecular weight < 500 Da can permeate the skin via the stratum corneum intercellular lipid lamellae. This is the most efficient diffusion route. PF201 has the highest molecular weight among the four test substances and the lowest log K ow. This could explain PF201's concentrations <LLOQ in most of our samples.

Skin metabolism is particularly important for chemicals with a high first-pass metabolism in the liver, e.g. BPA. After oral dosing in humans, 90% of the BPA dose undergoes first-pass metabolism and 10% of the dose enters the systemic circulation.[56] Our results show that BPA metabolism to BPA-G was negligible in *ex-vivo* human skin. These differences in metabolism between dermal and oral routes of exposures will likely result in higher bioavailability of BPA from dermal exposure despite the lower skin absorption compared to oral absorption.

A limitation of our study was that the analytical method was not developed to quantify the skin metabolism of BPS, D-8 and PF201. BPS metabolism in humans is known and is mainly phase II conjugation, as observed for BPA metabolism. We deemed conjugation by the skin negligible, which has recently been supported for BPS.[57] Thus, we did not add a deconjugation step. Our method could be further developed to include metabolites for all color developers, once data on D-8 and PF201 metabolism become available. Another limitation of our study was the higher acceptance criteria for LLOQ and QC solutions' accuracy and precision, compared to values recommended by guidelines on bioanalytical method validation. This was due to some critical points, namely the lower accuracy of BPA at low-QCs compared to BPA-G, BPS, D-8, and PF201, and the matrix effects on BPA and BPS. However, *in vitro* skin absorption experiments are characterized by a high variability due to inter-individual and intra-individual differences in the skin samples, which make our method fit for its intended purpose. Finally, this analytical method was developed for a matrix, i.e., saline that had been in contact with human dermis, but its applicability could potentially be widened to urine samples of human biomonitoring studies.

In summary, a sensitive LC-MS/MS method was developed and validated for the quantification of BPA, BPA-G and BPA alternatives used as color developers in thermal paper receipts. Our method was in line with guidelines of bioanalytical method validation [53] but with higher acceptance thresholds for LLOQ and QC accuracy and precision. Our method was robust for the analysis of samples from *in vitro* human skin absorption experiments, where the matrix was saline that had been in contact with human dermis for up to 24 h. In our preliminary *in vitro* assays, BPA and D-8 had the highest potential for human skin absorption, and BPA skin metabolism to BPA-G was negligible.

This project was funded by the SwISS Centre for Applied Human Toxicology (SCAHT) and the SwISS Federal Office of Public Health (FOPH). Authors have no competing interests to declare.

Acknowledgments. We acknowledge the Centre Hospitalier Universitaire Vaudois (CHUV, Lausanne, Switzerland) for providing the human skin samples.

The authors declare no competing financial interest.

References

(1) Chen, M.-Y.; Ike, M.; Fujita, M. Acute Toxicity, Mutagenicity, and Estrogenicity of Bisphenol-A and Other Bisphenols. *Environ. Toxicol.* **2002**, *17* (1), 80–86.

(2) Fic, A.; Žegura, B.; Gramec, D.; Mašič, L. P. Estrogenic and Androgenic Activities of TBBA and TBMEPH, Metabolites of Novel Brominated Flame Retardants, and Selected Bisphenols, Using the XenoScreen XL YES/YAS Assay. *Chemosphere* **2014**, *112*, 362–369. https://doi.org/10.1016/j.chemosphere.2014.04.080.

(3) Richter, C. A.; Birnbaum, L. S.; Farabollini, F.; Newbold, R. R.; Rubin, B. S.; Talsness, C. E.; Vandenbergh, J. G.; Walser-Kuntz, D. R.; vom Saal, F. S. In Vivo Effects of Bisphenol A in Laboratory Rodent Studies. *Reprod. Toxicol.* **2007**, *24* (2), 199–224. https://doi.org/10.1016/j.reprotox.2007.06.004.

(4) Wetherill, Y. B.; Akingbemi, B. T.; Kanno, J.; McLachlan, J. A.; Nadal, A.; Sonnenschein, C.; Watson, C. S.; Zoeller, R. T.; Belcher, S. M. In Vitro Molecular Mechanisms of Bisphenol A Action. *Reprod. Toxicol.* **2007**, *24* (2), 178–198. https://doi.org/10.1016/j.reprotox.2007.05.010.

(5) Liu, J.; Martin, J. W. Prolonged Exposure to Bisphenol A from Single Dermal Contact Events. *Environmental Science & Technology* **2017**, *51* (17), 9940–9949. https://doi.org/10.1021/acs.est.7b03093.

(6) Mendum, T.; Stoler, E.; VanBenschoten, H.; Warner, J. C. Concentration of Bisphenol A in Thermal Paper. *Green Chemistry Letters and Reviews* **2011**, *4* (1), 81–86. https://doi.org/10.1080/17518253.2010.502908.

(7) Porras, S. P.; Heinälä, M.; Santonen, T. Bisphenol A Exposure via Thermal Paper Receipts. *Toxicology Letters* **2014**, *230* (3), 413–420. https://doi.org/10.1016/j.toxlet.2014.08.020.

(8) Vervliet, P.; Gys, C.; Caballero-Casero, N.; Covaci, A. Current-Use of Developers in Thermal Paper from 14 Countries Using Liquid Chromatography Coupled to Quadrupole Time-of-Flight Mass Spectrometry. *Toxicology* **2019**, *416*, 54–61. https://doi.org/10.1016/j.tox.2019.02.003.

(9) von Goetz, N.; Pirow, R.; Hart, A.; Bradley, E.; Poças, F.; Arcella, D.; Lillegard, I. T. L.; Simoneau, C.; van Engelen, J.; Husoy, T.; Theobald, A.; Leclercq, C. Including Non-Dietary Sources into an Exposure Assessment of the European Food Safety Authority: The Challenge of Multi-Sector Chemicals Such as Bisphenol A. *Regulatory Toxicology and Pharmacology* **2017**, *85*, 70–78. https://doi.org/10.1016/j.yrtph.2017.02.004.

(10) Biedermann, S.; Tschudin, P.; Grob, K. Transfer of Bisphenol A from Thermal Printer Paper to the Skin. *Analytical and Bioanalytical Chemistry* **2010**, *398* (1), 571–576. https://doi.org/10.1007/s00216-010-3936-9.

(11) Ndaw, S.; Remy, A.; Denis, F.; Marsan, P.; Jargot, D.; Robert, A. Occupational Exposure of Cashiers to Bisphenol S via Thermal Paper. *Toxicol. Lett.* **2018**, *298*, 106–111. https://doi.org/10.1016/j.toxlet.2018.05.026.

(12) Ndaw, S.; Remy, A.; Jargot, D.; Robert, A. Occupational Exposure of Cashiers to Bisphenol A via Thermal Paper: Urinary Biomonitoring Study. *International Archives of Occupational and Environmental Health* **2016**, *89* (6), 935–946. https://doi.org/10.1007/s00420-016-1132-8.

(13) Björnsdotter, M. K.; Jonker, W.; Legradi, J.; Kool, J.; Ballesteros-Gómez, A. Bisphenol A Alternatives in Thermal Paper from the Netherlands, Spain, Sweden and Norway. Screening and Potential Toxicity. *Science of The Total Environment* **2017**, *601–602*, 210–221. https://doi.org/10.1016/j.scitotenv.2017.05.171.

(14) Eckardt, M.; Simat, T. J. Bisphenol A and Alternatives in Thermal Paper Receipts - a German Market Analysis from 2015 to 2017. *Chemosphere* **2017**, *186*, 1016–1025. https://doi.org/10.1016/j.chemosphere.2017.08.037.

(15) Goldinger, D. M.; Demierre, A.-L.; Zoller, O.; Rupp, H.; Reinhard, H.; Magnin, R.; Becker, T. W.; Bourqui-Pittet, M. Endocrine Activity of Alternatives to BPA Found in Thermal Paper in Switzerland. *Regulatory Toxicology and Pharmacology* **2015**, *71* (3), 453–462. https://doi.org/10.1016/j.yrtph.2015.01.002.

(16) Russo, G.; Barbato, F.; Grumetto, L. Monitoring of Bisphenol A and Bisphenol S in Thermal Paper Receipts from the Italian Market and Estimated Transdermal Human Intake: A Pilot Study. *Sci. Total Environ.* **2017**, *599–600*, 68–75. https://doi.org/10.1016/j.scitotenv.2017.04.192.

(17) Kuruto-Niwa, R.; Nozawa, R.; Miyakoshi, T.; Shiozawa, T.; Terao, Y. Estrogenic Activity of Alkylphenols, Bisphenol S, and Their Chlorinated Derivatives Using a GFP Expression System. *Environ. Toxicol. Pharmacol.* **2005**, *19* (1), 121–130. https://doi.org/10.1016/j.etap.2004.05.009.

(18) US EPA. *Bisphenol A Alternatives in Thermal Paper, Final Report.*; United States Environmental Protection Agency, 2014.

(19) Demierre, A.-L.; Peter, R.; Oberli, A.; Bourqui-Pittet, M. Dermal Penetration of Bisphenol A in Human Skin Contributes Marginally to Total Exposure. *Toxicology Letters* **2012**, *213* (3), 305–308. https://doi.org/10.1016/j.toxlet.2012.07.001.

(20) Marquet, F.; Payan, J.-P.; Beydon, D.; Wathier, L.; Grandclaude, M.-C.; Ferrari, E. In Vivo and Ex Vivo Percutaneous Absorption of [14C]-Bisphenol A in Rats: A Possible Extrapolation to Human Absorption? *Archives of Toxicology* **2011**, *85* (9), 1035–1043. https://doi.org/10.1007/s00204-011-0651-z.

(21) Mørck, T. J.; Sorda, G.; Bechi, N.; Rasmussen, B. S.; Nielsen, J. B.; Ietta, F.; Rytting, E.; Mathiesen, L.; Paulesu, L.; Knudsen, L. E. Placental Transport and in Vitro Effects of Bisphenol A. *Reproductive Toxicology* **2010**, *30* (1), 131–137. https://doi.org/10.1016/j.reprotox.2010.02.007.

(22) Toner, F.; Allan, G.; Dimond, S. S.; Waechter, J. M.; Beyer, D. In Vitro Percutaneous Absorption and Metabolism of Bisphenol A (BPA) through Fresh Human Skin. *Toxicol In Vitro* **2018**, *47*, 147–155. https://doi.org/10.1016/j.tiv.2017.11.002.

(23) Zalko, D.; Jacques, C.; Duplan, H.; Bruel, S.; Perdu, E. Viable Skin Efficiently Absorbs and Metabolizes Bisphenol A. *Chemosphere* **2011**, *82* (3), 424–430. https://doi.org/10.1016/j.chemosphere.2010.09.058.

(24) Snyder, R. W.; Maness, S. C.; Gaido, K. W.; Welsch, F.; Sumner, S. C.; Fennell, T. R. Metabolism and Disposition of Bisphenol A in Female Rats. *Toxicol. Appl. Pharmacol.* **2000**, *168* (3), 225–234. https://doi.org/10.1006/taap.2000.9051.

(25) Zhou, X.; Kramer, J. P.; Calafat, A. M.; Ye, X. Automated On-Line Column-Switching High Performance Liquid Chromatography Isotope Dilution Tandem Mass Spectrometry Method for the Quantification of Bisphenol A, Bisphenol F, Bisphenol S, and 11 Other Phenols in Urine. *Journal of Chromatography B* **2014**, *944*, 152–156. https://doi.org/10.1016/j.jchromb.2013.11.009.

(26) Skledar, D. G.; Schmidt, J.; Fic, A.; Klopčič, I.; Trontelj, J.; Dolenc, M. S.; Finel, M.; Mašič, L. P. Influence of Metabolism on Endocrine Activities of Bisphenol S. *Chemosphere* **2016**, *157*, 152–159. https://doi.org/10.1016/j.chemosphere.2016.05.027.

(27) Liu, J.; Martin, J. W. Comparison of Bisphenol A and Bisphenol S Percutaneous Absorption and Biotransformation. *Environ. Health Perspect.* **2019**, *127* (6), 67008. https://doi.org/10.1289/EHP5044.

(28) Huysman, S.; Van Meulebroek, L.; Janssens, O.; Vanryckeghem, F.; Van Langenhove, H.; Demeestere, K.; Vanhaecke, L. Targeted Quantification and Untargeted Screening of Alkylphenols, Bisphenol A and Phthalates in Aquatic Matrices Using Ultra-High-Performance Liquid Chromatography Coupled to Hybrid Q-Orbitrap Mass Spectrometry. *Anal. Chim. Acta* **2019**, *1049*, 141–151. https://doi.org/10.1016/j.aca.2018.10.045.

(29) Lee, S.; Kim, C.; Youn, H.; Choi, K. Thyroid Hormone Disrupting Potentials of Bisphenol A and Its Analogues - in Vitro Comparison Study Employing Rat Pituitary (GH3) and Thyroid Follicular (FRTL-5) Cells. *Toxicology in Vitro* **2017**, *40*, 297–304. https://doi.org/10.1016/j.tiv.2017.02.004.

(30) Thayer, K. A.; Taylor, K. W.; Garantziotis, S.; Schurman, S.; KISSling, G. E.; Hunt, D.; Herbert, B.; Church, R.; Jankowich, R.; Churchwell, M. I.; Scheri, R. C.; Birnbaum, L. S.; Bucher, J. R. Bisphenol A, Bisphenol S, and 4-Hydroxyphenyl 4-Isoprooxyphenylsulfone (BPSIP) in Urine and Blood of Cashiers. *Environmental Health Perspectives* **2015**. https://doi.org/10.1289/ehp.1409427.

(31) Van Overmeire, I.; Vrijens, K.; Nawrot, T.; Van Nieuwenhuyse, A.; Van Loco, J.; Reyns, T. Simultaneous Determination of Parabens, Bisphenols and Alkylphenols in Human Placenta by Ultra-High Performance Liquid Chromatography-Tandem Mass Spectrometry. *J. Chromatogr. B Analyt. Technol. Biomed. Life Sci.* **2019**, *1121*, 96–102. https://doi.org/10.1016/j.jchromb.2019.05.012.

(32) Ye, X.; Kuklenyik, Z.; Needham, L. L.; Calafat, A. M. Measuring Environmental Phenols and Chlorinated Organic Chemicals in Breast Milk Using Automated On-Line Column-Switching–High Performance Liquid Chromatography–Isotope Dilution Tandem Mass Spectrometry. *Journal of Chromatography B* **2006**, *831* (1–2), 110–115. https://doi.org/10.1016/j.jchromb.2005.11.050.

(33) Andra, S. S.; Austin, C.; Yang, J.; Patel, D.; Arora, M. Recent Advances in Simultaneous Analysis of Bisphenol A and Its Conjugates in Human Matrices: Exposure Biomarker Perspectives. *Sci. Total Environ.* **2016**, *572*, 770–781. https://doi.org/10.1016/j.scitotenv.2016.07.062.

(34) Teeguarden, J. G.; Calafat, A. M.; Ye, X.; Doerge, D. R.; Churchwell, M. I.; Gunawan, R.; Graham, M. K. Twenty-Four Hour Human Urine and Serum Profiles of Bisphenol A during High-Dietary Exposure. *Toxicol Sci* **2011**, *123* (1), 48–57. https://doi.org/10.1093/toxsci/kfr160.

(35) Yao, Y.; Shao, Y.; Zhan, M.; Zou, X.; Qu, W.; Zhou, Y. Rapid and Sensitive Determination of Nine Bisphenol Analogues, Three Amphenicol Antibiotics, and Six Phthalate Metabolites in Human Urine Samples Using UHPLC-MS/MS. *Anal Bioanal Chem* **2018**, *410* (16), 3871–3883. https://doi.org/10.1007/s00216-018-1062-2.

(36) Yang, Y.; Yang, Y.; Zhang, J.; Shao, B.; Yin, J. Assessment of Bisphenol A Alternatives in Paper Products from the Chinese Market and Their Dermal Exposure in the General Population. *Environ. Pollut.* **2019**, *244*, 238–246. https://doi.org/10.1016/j.envpol.2018.10.049.

(37) García-Prieto, A.; Lunar, M. L.; Rubio, S.; Pérez-Bendito, D. Determination of Urinary Bisphenol A by Coacervative Microextraction and Liquid Chromatography–Fluorescence Detection. *Analytica Chimica Acta* **2008**, *630* (1), 19–27. https://doi.org/10.1016/j.aca.2008.09.060.

(38) Li, Q.; Wang, X.; Yuan, D. Preparation of Solid-Phase Microextraction Fiber Coated with Single-Walled Carbon Nanotubes by Electrophoretic Deposition and Its Application in Extracting Phenols from Aqueous Samples. *Journal of Chromatography A* **2009**, *1216* (9), 1305–1311. https://doi.org/10.1016/j.chroma.2008.12.082.

(39) Zarzycki, P. K.; Włodarczyk, E.; Baran, M. J. Determination of Endocrine Disrupting Compounds Using Temperature-Dependent Inclusion Chromatography. *Journal of Chromatography A* **2009**, *1216* (44), 7602–7611. https://doi.org/10.1016/j.chroma.2009.03.067.

(40) Chesher, D. Evaluating Assay Precision. *Clin Biochem Rev* **2008**, *29* (Suppl 1), S23–S26.

(41) Matuszewski, B. K.; Constanzer, M. L.; Chavez-Eng, C. M. Strategies for the Assessment of Matrix Effect in Quantitative Bioanalytical Methods Based on HPLC-MS/MS. *Anal. Chem.* **2003**, *75* (13), 3019–3030.

(42) OECD. Organisation for Economic Co-Operation and Development, Guidelines for the Testing of Chemicals, Section 4, Test N^{o} 428: Skin Absorption: In Vitro Method; 2004.

(43) Pinnagoda, J.; Tupker, R. A.; Agner, T.; Serup, J. Guidelines for Transepidermal Water Loss (TEWL) Measurement. A Report from the Standardization Group of the European Society of Contact Dermatitis. *Contact Derm.* **1990**, *22* (3), 164–178. https://doi.org/10.1111/j.1600-0536.1990.tb01553.x.

(44) Yang, Y.; Guan, J.; Yin, J.; Shao, B.; Li, H. Urinary Levels of Bisphenol Analogues in Residents Living near a Manufacturing Plant in South China. *Chemosphere* **2014**, *112*, 481–486. https://doi.org/10.1016/j.chemosphere.2014.05.004.

(45) Furey, A.; Moriarty, M.; Bane, V.; Kinsella, B.; Lehane, M. Ion Suppression; a Critical Review on Causes, Evaluation, Prevention and Applications. *Talanta* **2013**, *115*, 104–122. https://doi.org/10.1016/j.talanta.2013.03.048.

(46) Tan, D.; Jin, J.; Wang, L.; Zhao, X.; Guo, C.; Sun, X.; Dhanjai, null; Lu, X.; Chen, J. Ammonium Hydroxide Enhancing Electrospray Response and Boosting Sensitivity of Bisphenol A and Its Analogs. *Talanta* **2018**, *182*, 590–594. https://doi.org/10.1016/j.talanta.2018.02.033.

(47) Twaddle, N. C.; Churchwell, M. I.; Vanlandingham, M.; Doerge, D. R. Quantification of Deuterated Bisphenol A in Serum, TISSues, and Excreta from Adult Sprague-Dawley Rats Using Liquid Chromatography with Tandem Mass Spectrometry. *Rapid Commun. Mass Spectrom.* **2010**, *24* (20), 3011–3020. https://doi.org/10.1002/rcm.4733.

(48) Ye, X.; Zhou, X.; Hennings, R.; Kramer, J.; Calafat, A. M. Potential External Contamination with Bisphenol A and Other Ubiquitous Organic Environmental Chemicals during Biomonitoring Analysis: An Elusive Laboratory Challenge. *Environ. Health Perspect.* **2013**, *121* (3), 283–286. https://doi.org/10.1289/ehp.1206093.

(49) Vandenberg, L. N.; Gerona, R. R.; Kannan, K.; Taylor, J. A.; van Breemen, R. B.; Dickenson, C. A.; Liao, C.; Yuan, Y.; Newbold, R. R.; Padmanabhan, V.; vom Saal, F. S.; Woodruff, T. J. A Round Robin Approach to the Analysis of Bisphenol a (BPA) in Human Blood Samples. *Environ Health* **2014**, *13*, 25. https://doi.org/10.1186/1476-069X-13-25.

(50) vom Saal, F. S.; Welshons, W. V. Evidence That Bisphenol A (BPA) Can Be Accurately Measured without Contamination in Human Serum and Urine, and That BPA Causes Numerous Hazards from Multiple Routes of Exposure. *Molecular and Cellular Endocrinology* **2014**, *398* (1–2), 101–113. https://doi.org/10.1016/j.mce.2014.09.028.

(51) Matuszewski, B. K. Standard Line Slopes as a Measure of a Relative Matrix Effect in Quantitative HPLC-MS Bioanalysis. *J. Chromatogr. B Analyt. Technol. Biomed. Life Sci.* **2006**, *830* (2), 293–300. https://doi.org/10.1016/j.jchromb.2005.11.009.

(52) ICH. International Council for Harmonisation (ICH), Bioanalytical Method Validation M10; ICH Harmonised Guideline; 2018; p 63.

(53) FDA, U. S. F. & D. A. Bioanalytical Method Validation Guidance for Industry. **2018**, 44.

(54) Ye, X.; Bishop, A. M.; Reidy, J. A.; Needham, L. L.; Calafat, A. M. Temporal Stability of the Conjugated Species of Bisphenol A, Parabens, and Other Environmental Phenols in Human Urine. *J Expos Sci Environ Epidemiol* **2007**, *17* (6), 567–572. https://doi.org/10.1038/sj.jes.7500566.

(55) Guy, R. H.; Potts, R. O. Penetration of Industrial Chemicals across the Skin: A Predictive Model. *Am. J. Ind. Med.* **1993**, *23* (5), 711–719. https://doi.org/10.1002/ajim.4700230505.

(56) Gundert-Remy, U.; Mielke, H.; Bernauer, U. Commentary: Dermal Penetration of Bisphenol A—Consequences for Risk Assessment. *Toxicology Letters* **2013**, *217* (2), 159–161. https://doi.org/10.1016/j.toxlet.2012.12.009.

(57) Champmartin, C.; Marquet, F.; Chedik, L.; Décret, M.-J.; Aubertin, M.; Ferrari, E.; Grandclaude, M.-C.; Cosnier, F. Human in Vitro Percutaneous Absorption of Bisphenol S and Bisphenol A: A Comparative Study. *Chemosphere* **2020**, *252*, 126525. https://doi.org/10.1016/j.chemosphere.2020.126525.